SCIENCE CHINA
Information Sciences

• RESEARCH PAPER •

July 2012 Vol. 55 No. 7: 1509–1519
doi: 10.1007/s11432-011-4467-5

Radiance-based color calibration for image-based modeling with multiple cameras

ZHAO Xu[1,2], ZHOU Zhong[1,2*] & WU Wei[1,2]

[1]*State Key Laboratory of Virtual Reality Technology and Systems, Beihang University, Beijing* 100191*, China;*
[2]*School of Computer Science and Engineering, Beihang University, Beijing* 100191*, China*

Received February 17, 2011; accepted May 18, 2011; published online April 12, 2012

Abstract Photo-consistency estimation is an important part for many image-based modeling techniques. This paper presents a novel radiance-based color calibration method to reduce the uncertainty of photo-consistency estimation across multiple cameras. The idea behind our method is to convert colors into a uniform radiometric color space in which multiple image data are corrected. Experimental results demonstrate that our method can achieve comparable color calibration effect without adjusting camera parameters and is more robust than other existing method. Additionally, we obtain an auto-determined threshold for photo-consistency check, which will lead to a better performance than existing photo-consistency based reconstruction algorithms.

Keywords color calibration, photo-consistency estimation, multi-camera system, image-based modeling

Citation Zhao X, Zhou Z, Wu W. Radiance-based color calibration for image-based modeling with multiple cameras. Sci China Inf Sci, 2012, 55: 1509–1519, doi: 10.1007/s11432-011-4467-5

1 Introduction

The development of low-cost acquiring devices and increasing popularity of multi-camera vision systems are continuously escalating image-based modeling applications [1,2]. One kind of attractive applications is to well reconstruct the real scene or object with multiple images [3,4]. Although multiple images can be manually captured with a hand-held camera [5] or automatically using a turntable or robot based system [6,7], they all suffer from a difficulty in modeling dynamic scenes. Unlike that, multi-camera vision systems have been emerged as a popular platform for providing effective support for applications with real-time requirement. However, it faces the challenge of how to decrease the influence introduced by the differences between cameras, which might further affect many photo-consistency based reconstruction algorithms [8,9]. Figure 1(b) and (c) illustrate some typical artifacts occurring in space carving reconstruction caused by the inconsistency of color matching costs, even if camera settings and types are virtually the same.

As mentioned in [10], different cameras-even if they are of the same type-do not exhibit consistent response. Furthermore, camera responses may differ in settings, illuminations and so on. A direct and effective method to eliminate these differences is to adjust camera settings to make their responses sim-

*Corresponding author (email: zz@vrlab.buaa.edu.cn)

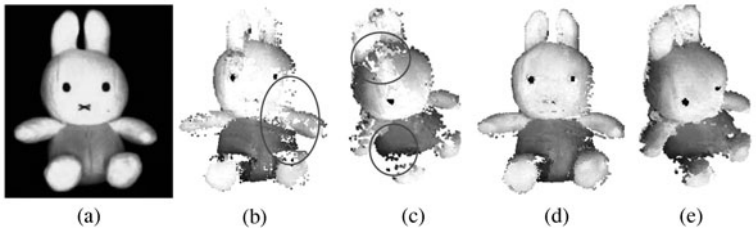

Figure 1 Space carving [8] reconstruction of a rabbit toy from six different views. (a) One of input toy rabbit images. (b)(c) A reconstruction using uncalibrated cameras with same settings. The artifacts are marked by circles. (d)(e) A reconstruction after color calibration. The artifacts are eliminated.

ilar [11]. It assumes that cameras are adjustable and can be physically accessed by calibration system. Consequently it is not suitable for many low-end acquiring devices.

Besides, color consistency can also be achieved by software processing of multiple images. Porikli [12] explicitly models pair-wise transfer functions between images, and uses these functions to correct multiple images. Although it shows consistent appearances, it is ineligible to guarantee numerical consistency for ignoring differences between cameras. This would yield a poor reconstructed model with unwanted artifacts, such as "outlier" or "gap" marked by circles in Figure 1(b) and (c).

Our goal is to achieve color consistency across multiple cameras so as to reduce matching noise for photo-consistency estimation. The key idea here is to map all captured image data from multiple cameras into a uniform radiometric color space and then correct them with estimated transformation matrices to one manually or automatically selected image. After our color calibration, images are consistent both visually and numerically. Photo-consistency based reconstruction algorithms can produce more reasonable results, shown in Figure 1(d) and (e).

The remainder of this paper is organized as follows: Section 2 presents the related work. Section 3 discusses the motivation for our work. The detailed radiance-based color calibration method is described in Section 4. Section 5 shows experiment results and evaluates photo-consistency measurements which are further applied in 3D reconstruction applications. Finally, further steps are discussed in conclusions.

2 Related work

The direct way to perform color calibrate across multiple cameras is to repeatedly adjust camera parameters (such as gain and brightness) until all the camera responses are similar enough to each other. Nanda et al. [11] use scene statistics as feedback to adjust the parameters of multiple cameras in their RingCam system. The main drawback of this method is that the acquiring devices must be physically accessible and it is not applicable for many low-end acquiring devices.

Furthermore, several software post processing techniques are proposed. Joshi [13] fits the response function as linear function, while Ilie [10] tries to minimize a cost function among images by adjusting hardware parameters. Based on their original work, Malik [14] uses a neural network based transform to optimize the software correction process, while Yamamoto [15] uses scale invariant feature transform to detect correspondences instead of a color chart board. However, all methods above need to perform hardware parameter adjustment at first. In contrast, our method does not need to adjust camera parameters but finally produces consistent colors both visually and numerically.

Another way to achieve color consistency across multiple cameras is by software processing of captured images. Porikli [12] designs a method based on image color histograms to modeling transfer functions and pair-wise correct multiple images. However, this method is difficult to ensure numerical color consistency for ignoring physical differences between cameras, and it may cause distortions and quantization errors when some parts of color spectrum are compressed or stretched. In our method, we first try to eliminate the above noise for each camera and then perform color correction with multiple images. Moreover, we address more attention to the issue of photo-consistency estimation and discuss the application of color calibration for image-based modeling.

To sum up, the characteristics of our method are in three aspects:

(1) Radiance-based color calibration. A uniform radiometric color space is defined for color correction with multiple images. We argue that such space is a camera-independent linear space and show that photo-consistency estimation will benefit from our radiance-based color calibration.

(2) Hardware-based configuration free. Unlike other multi-camera color calibration methods, our method shows comparable color calibration effect without obtaining and adjusting any camera parameters. It is much easier for our method to incorporate with unknown capturing devices.

(3) Auto-determined threshold for photo-consistency check. Through statistically analyzing photo-consistency matching costs of color chart images, we find that matching at the white color will yield the largest cost value. It helps us to automatically determine the photo-consistency check threshold instead of setting them tentatively.

3 Motivation

Essentially, color calibration methods are closely related to the color imaging process. Based on this, we classify these methods into three levels and define a uniform radiometric color space for color calibration.

Note that the definition of calibration varies in different areas. Here the term is typically used to describe a correction process of turning a general model of the physical device to a standard specific instance. Geometric calibration makes sure that all pinhole camera models reach geometry consistency in the sense of projective, affine, or Euclidean geometry, while color calibration ensures color consistency across multiple cameras at certain level in color imaging process. Different manufacturers usually implement this process in different ways. However, in theory, it is possible to statistically model color imaging process by a general polynomial function [16]. Inspired by this empirical model, we show three different color calibration levels on the basis of color imaging process in Figure 2.

The whole color imaging process consists of four sequential phases: (1) sensing and sampling spectral irradiance, (2) color-space and white-balance transforming, (3) nonlinear color rendering, and (4) image encoding. In this pipeline, color can be measured and expressed in different forms, such as irradiance, raw data, colorimetric tristimulus values or image pixels. Accordingly, color calibration can be performed within any color space at any level.

Different level color calibrations may yield different results. Since the lower level method puts more emphasis on differences between cameras, it will produce more consistent color calibration results. However, we find that it is not always necessary to calibrate all cameras at as lowest level as possible. According to the experimental results in [16], the first two phases of color imaging can be approximately modeled as a linear operator, which means that colorimetric tristimulus values are linearly related to image irradiance and scene radiance (assuming one compensates for optical effects like vignetting). Moreover, the main differences between different camera types lie in the third nonlinear color rendering phase. Therefore, we use colorimetric tristimulus values to define the uniform radiometric color space which can be seen as approximately linear and camera-independent space. That is the original reason why we choose to calibrate all cameras in this uniform radiometric color space at the middle level.

4 Multi-camera color calibration process

Our color calibration consists of two main phases: response function and transformation matrix recovery phase and multi-image color correction phase. The first phase helps us to map all captured image data from multiple cameras into the uniform radiometric color space described in Section 3. Transformation matrices are then saved for the second color correction phase. Finally, pixel value truncation problem and photo-consistency estimation issue are discussed.

Figure 3 shows an overview of our method, which proceeds in six steps:

Step 1. Recover the response function from five images with different exposures and select the target image with the largest gamut range.

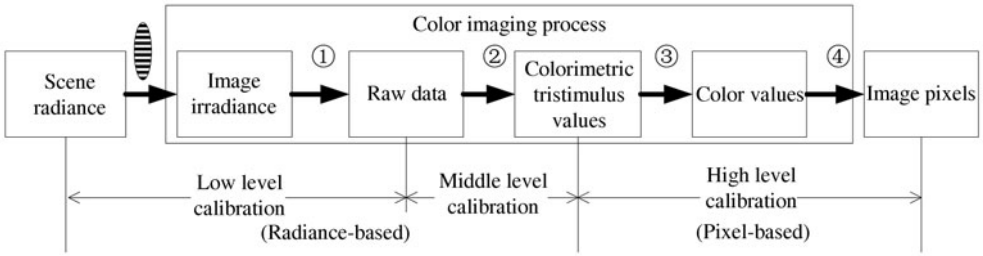

Figure 2 Color calibration levels on the basis of color imaging process [16]. Our radiance-based color calibration method lies in the middle level, which does not need to adjust camera parameters like low level calibration, but obtains a more consistent result than pixel-based calibration.

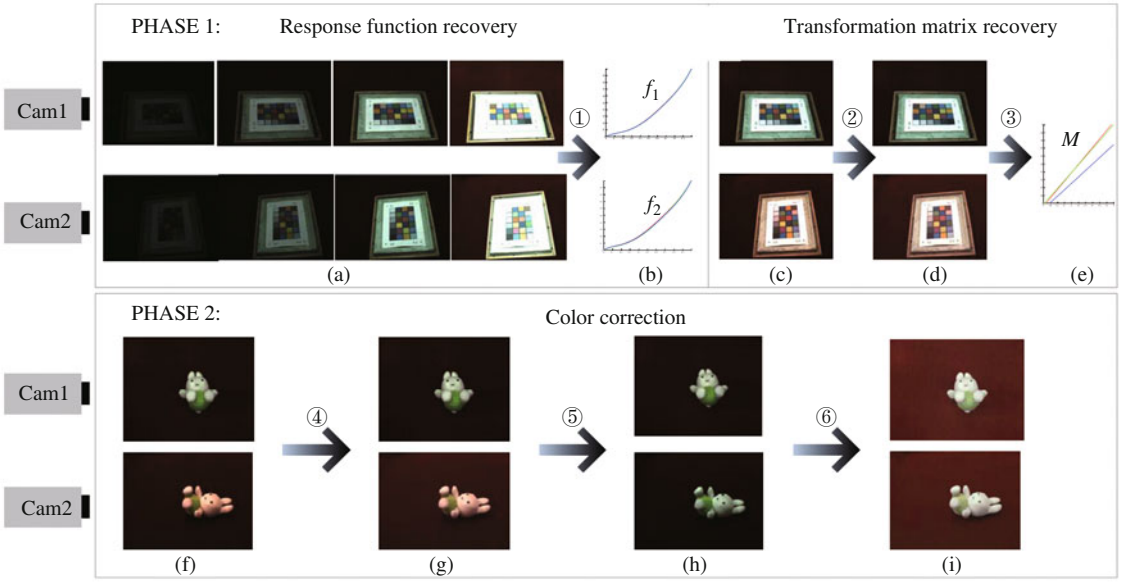

Figure 3 The overview of our multi-camera color calibration method, taking two cameras color calibrating for example. The image captured by "Cam1" is simply selected as target image here. The upper row (a)–(e) shows the response function and transformation matrix recovery phase, followed by color correction phase shown in lower row (f)–(i). In the first phase, two sets of images with varying exposures (a) are inputted to calculate the response curves (b). Color chart images under different camera settings (c) are inversely mapped by the response functions. Outputs (d) are then used to estimate the coefficient matrix (e) by least squares matching. In the second phase, Rabbit toy images captured by the same cameras (f) are inversely mapped to images (g) by the recovered response functions, and then corrected by linear transformation. Calibrated images (h) can also be processed by a new response function for better appearances (i).

Step 2. Locate the color chart board by geometric calibration, sample 24 colors and inversely map them with the previous response function.

Step 3. Estimate the coefficient vectors or matrix and save both response functions and transformation matrices for the next phase.

Step 4. Process images of reconstructed scene with the corresponding recovered response function.

Step 5. Correct all the images by the estimated transformation matrices.

Step 6. Apply a new response function for better appearances if needed. More details are described in the following subsections.

4.1 Response function and transformation matrix recovery

Researchers have proposed several methods to calculate the response function for a single camera. The most popular methods involve taking multiple registered images of a static scene with varying camera exposures [17] or illuminations [18]. The basic idea of these methods is to fully use statistics of images

with different exposures or illuminations and then to fit them into an empirical mathematical polynomial function. Lin et al. present a novel response estimation method by exploiting intensity statistics at edges [19]. We simply choose Mitsunaga's RASCAL software [20] to calculate response functions of all cameras one by one for its robustness. The recovered function curves are shown in Figure 3(b). All images captured in this phase contain the same GretagMacbeth ColorChecker$^{\mathrm{TM}}$ chart [21] for color sampling.

Instead of explicitly adjusting camera configurations, we have to carefully select the target image which others correct to. If the target image has a limited gamut range, say too dark or too bright, the corrected images may introduce distortions and quantization errors. So we search for all candidate images and select the one which is both visually good and has the largest gamut range. This can be automatically done by analyzing the range of 24 sampled colors. It is possible that no image satisfies the condition. In this case, we generate a high dynamic range image from images with different exposures by RASCAL, and then equalize it as the standard target.

After being inversely mapped to radiometric color space, the sampled colors are then used to model the transfer function between the target image and each candidate image. Similar to [10], we estimate the transformation matrix in two ways: linear least squares matching and a 3×3 RGB to RGB transformation. The complicated general polynomial transformation is not necessary, since we explicitly compensate the nonlinearities of camera response functions.

The linear squares matching is the simplest and fastest method to estimate the coefficient matrix. It minimizes the following function in least square sense:

$$\sum_{i=1}^{N}((a_c\boldsymbol{I}_{ci}+b_c)-\boldsymbol{T}_{ci})^2,\quad c\in\{r,g,b\},\tag{1}$$

where $\boldsymbol{I}$ and $\boldsymbol{T}$ refer to the color vectors in candidate and target images. We use $N=24$ samples to fit this function. A disadvantage is that linear squares matching scales and translates the color values of each channel independently and ignores the inter-channel effects. Ilie [10] suggests using a 3×3 RGB to RGB transformation matrix to improve it, which is the solution to the following over-constrained system:

$$\sum_{i=1}^{N}(\boldsymbol{I}_{ci}\cdot\boldsymbol{M}_{3\times3}-\boldsymbol{T}_{ci})=\boldsymbol{0},\quad c\in\{r,g,b\}.\tag{2}$$

We solve the problem of estimating matrix $\boldsymbol{M}_{3\times3}$ using singular value decomposition. Here the coefficient vectors a and b in Eq. (3) and matrix $\boldsymbol{M}_{3\times3}$ in Eq. (4) are calculated and saved for the next color correction phase.

4.2 Color correction

The second phase's goal is to correct multiple candidate images to the target one. With the same setting to the previous phase, we capture a set of new images which contain the scene or object to be reconstructed, as the input of the second phase.

The general formula of color correction can be written as

$$\boldsymbol{P}'_c=a_c\cdot f_c^{-1}(\boldsymbol{P}_c)+b_c,\quad c\in\{r,g,b\},\tag{3}$$

or

$$\boldsymbol{P}'_c=\boldsymbol{M}_{3\times3}\cdot f_c^{-1}(\boldsymbol{P}_c),\quad c\in\{r,g,b\}.\tag{4}$$

Eqs. (3) and (4) respectively describe two color correction processes by least squares matching and 3×3 RGB to RGB transformation, where $\boldsymbol{P}_c$ and $\boldsymbol{P}'_c$ represent the pixel values before and after correction. In theory, color correction by 3×3 RGB to RGB transformation should yield a better result than the correction by linear squares matching, but in our method we find that both methods produce nearly the same results. Calibrated images are shown in Figure 3(h). In some cases, these images may be too dark for observing. A new uniform response function is proposed to improve it (making gamma equal to 2.2 for example). Results are illustrated in Figure 3(i).

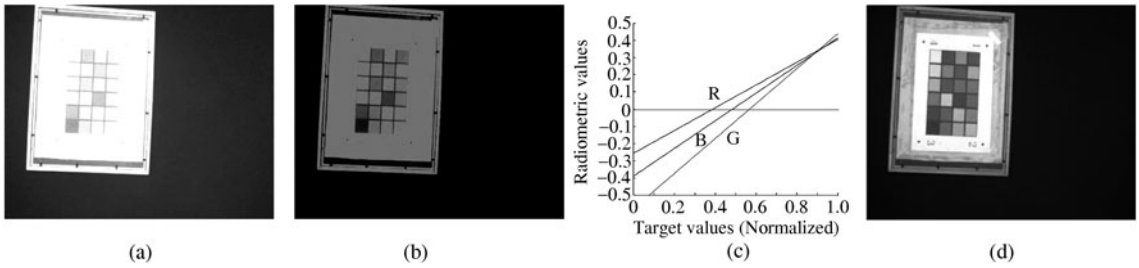

Figure 4 Truncation problem example and analysis. (a) The over-exposure input image; (b) corrected image with background pixels are truncated; (c) the least squares fitted lines of RGB channels. Note that the left-half part of each line is below zero. (d) Truncation problem resolved by Ilie's method [10].

4.3 Truncation problem

Truncation problem may occur when the input image is too dark or too bright as shown in Figure 4(a). This is because background pixel values are beyond the range of sampled 24 colors. Any correction methods cannot recover these colors when sampling range is too narrow. The left-half part of each fitted line shown in Figure 4(c) is below zero, which yields meaningless pixels.

We then use statistic method to make analysis when our color calibration method can be correctly used. Since the white color is expressed by red, green and blue components with max values, we choose the variance of white color to predict whether the truncation problem would occur. We observe that when the image is too dark (the RMSE value of white color is more than 200), our calibration method cannot work correctly or with lots of noise. On the other hand, when the image is too bright (the RMSE value of white color is less than the RMSE values of other colors), the truncation problem will happen again. This can be automatically done to decide whether our method can be correctly used. In practice, users can roughly adjust camera parameters to ensure they can distinguish black from dark grey or white from light grey. Then, our method can further calibrate colors and achieve photo-consistency.

4.4 Photo-consistency estimation

Photo-consistency based reconstruction algorithms need a threshold which distinguishes the consistent matches from the inconsistent matches. It is always determined by trial and error. We explicitly measure and determine it by projecting the sampled points on color chart board back to images, computing the matching costs and choosing the maximum value as threshold. In the next section, we argue that matching at the white color will yield the largest cost value.

5 Experimental results

For experiment purposes, we set up a multi-camera acquiring platform shown in Figure 5(a). Cameras can be fixed in the platform at arbitrary positions. The color chart board or objects to be reconstructed are placed in the center to make sure all cameras can observe them. A synchronized multi-camera acquiring system is developed and deployed on PCs. Multiple cameras are firstly calibrated by Bouguet's geometric calibration toolbox [22]. Then the color chart board with markers is located to obtain color sample 3D position. Figure 5(b) illustrates calibrated extrinsic parameters and camera IDs.

5.1 Comparison before and after color calibration

Firstly, we use six Flea2 cameras provided by PointGrey, Inc. [23] with the same settings and capture a toy rabbit for an implementation of space carving 3D reconstruction algorithm presented in [8]. The threshold here is set to 20 by trial and error.

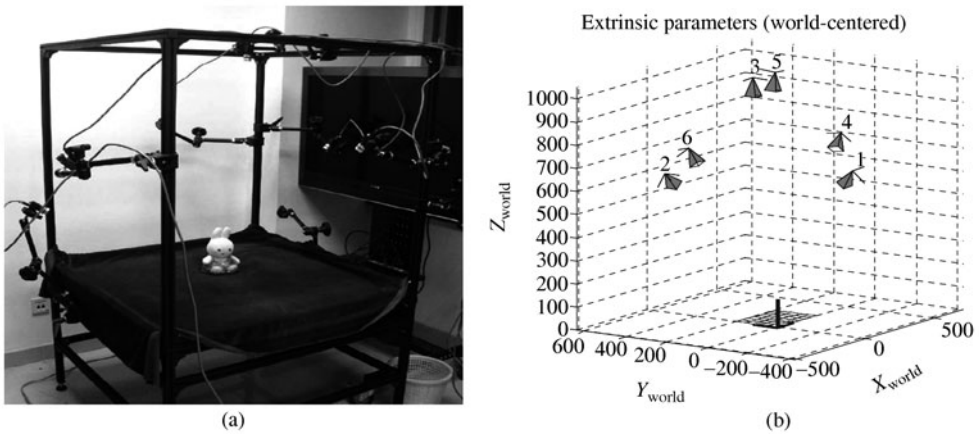

Figure 5 Multi-camera acquiring system and camera distributions. (a) The acquiring platform with six fixed cameras; (b) visualization of extrinsic parameters after geometric calibration.

Table 1 Different settings of six cameras

CameraID	Acquisition case	Shutter(ms)	Exposure(EV)	White balance(R/B)
1	As standard	100	0.38	550/650
2	Tend to dark	41.8	−1	550/650
3	Tend to bright	110	0.45	550/650
4	Tend to warm	100	0.38	680/650
5	Tend to cool	100	0.38	550/760
6	AVT Marlin 046C [24]	Shutter=1000; Gain=0; WB=75/72; Gamma=1.0		

In our first experiment, camera types and settings are all the same (the standard acquistion case as shown in Table 1). However the estimated photo-consistency matching costs still contain too much noise which yields artifacts as shown in Figure 1(b) and (c). After our color calibration, the reconstruction results (Figure 1(d) and (e)) are improved and noticeable artifacts marked in circles are eliminated.

We made a second experiment using multiple cameras with different settings and types. The configurations are listed in Table 1. The six images captured by these cameras are given in Figure 6. Figure 7 shows the corrected images after our color calibration.

Comparing with Figure 6 and Figure 7, we find that all candidate images are color consistent to the target image (Figure 6(a)) after color calibration. It proves that our multi-camera color calibration method is effective when cameras have different settings like exposures (by adjusting aperture, gain or shutter time), white balances and even different types (mainly different response functions).

We have also compared our method with Ilie's and Porikli's methods under the same camera configurations listed in Table 1. Here we use 3×3 RGB to RGB transformation as color correction method and use the mean inter-sample standard deviations to measure the color consistency. Table 2 shows the comparison results. Both Ilie's and our methods greatly reduce these values and achieve color consistency numerically and Ilie's method is better than ours. However, results are so close that difference can be ignored when compared to Porikli's method. Moreover, we do not need to adjust any camera parameters. Porikli's results seem bad in the figures. The main reason is that part of the pixels are truncated during calibration.

Figure 8 shows sampled color distributions of input images before and after color calibration. The measured color values approximately converge to a straight line. Note that the largest variation happens when RGB values are the largest. It means that the white color has the maximum uncertainty, which will be clearly shown in the next experiment.

5.2 Photo-consistency based multiview reconstruction

We further compute photo-consistency matching costs of 24 sampled colors across multiple cameras before and after color calibration. Here we choose RMSE (root mean square error) and SAD (sum of absolute

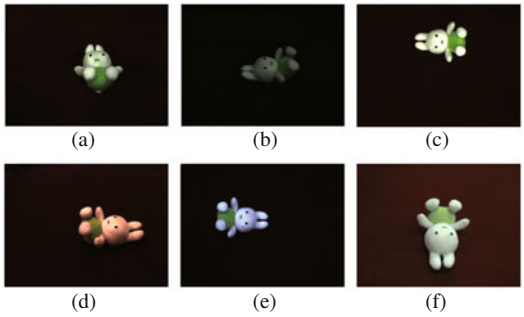

Figure 6 Six images captured with different camera settings and types. They visually look different. (a) normal; (b) dark; (c) bright; (d) warm; (e) cool. Image (f) is captured by another type of camera.

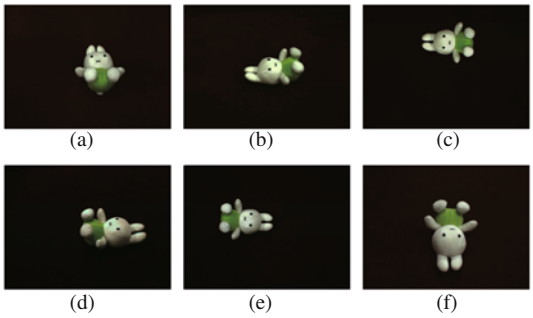

Figure 7 Six images corrected by our color calibration. Images (b)–(f) are visually color consistent to the target image (a) after our color calibration.

Table 2 Comparison between our, Ilie's and Porikli's color calibration methods

	Channel	Before calibrated	Our method	Ilie's method [10]	Porikli's method [12]
Mean	R	42.2093	3.9834	2.9864	37.2798
inter-sample	G	39.7660	3.5263	2.3681	36.0696
st. dev.	B	42.5107	5.5870	3.1840	39.4626

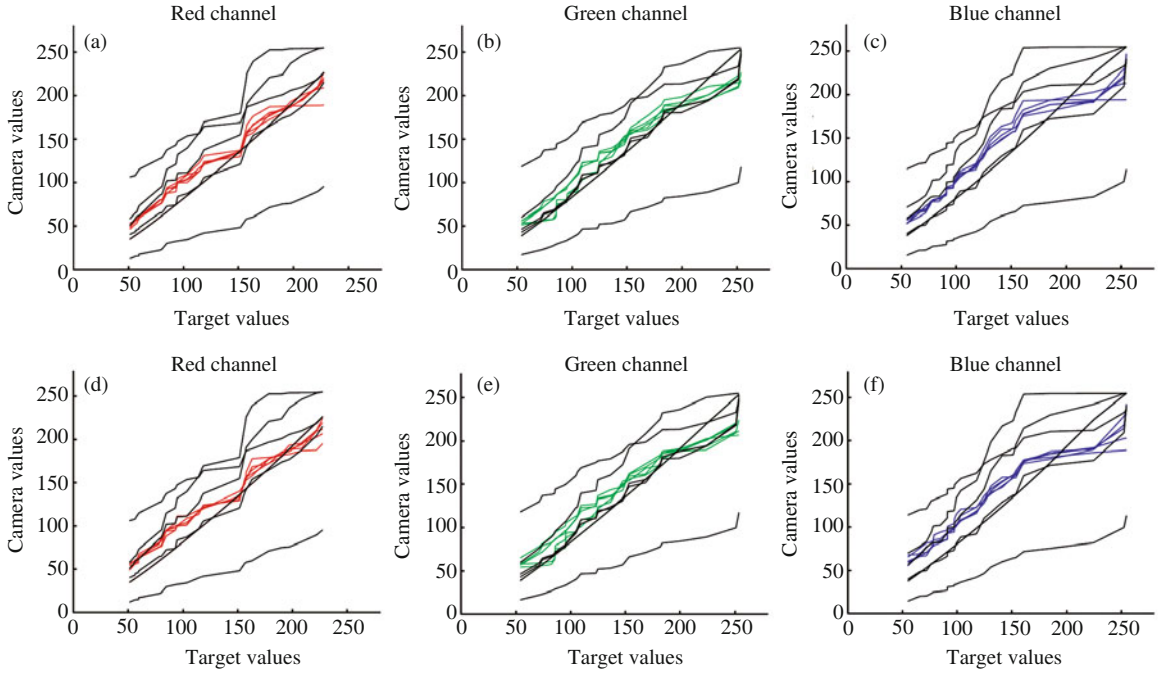

Figure 8 The measured color for each channel, camera and sample, plotted with respect to the corresponding target values. The six black lines in each figure represent the sampled color distributions of six images in Figure 6. The red, green and blue lines represent the corrected color distributions of six images in Figure 7. The upper three figures (a)–(c) show the corrected results by linear squares matching. The lower three figures (d)–(f) show the corrected results by 3×3 RGB to RGB transformation. Both linear squares matching and 3×3 RGB to RGB transformation yield nearly the same convergence results.

difference), two classic distance-based similarity measurements for image-based modeling, as matching cost functions. The comparison is shown in Figure 9.

After color calibration, the RMSE and SAD photo-consistency matching cost values as well as variations become significantly smaller. Both linear least squares matching and RGB to RGB transformation

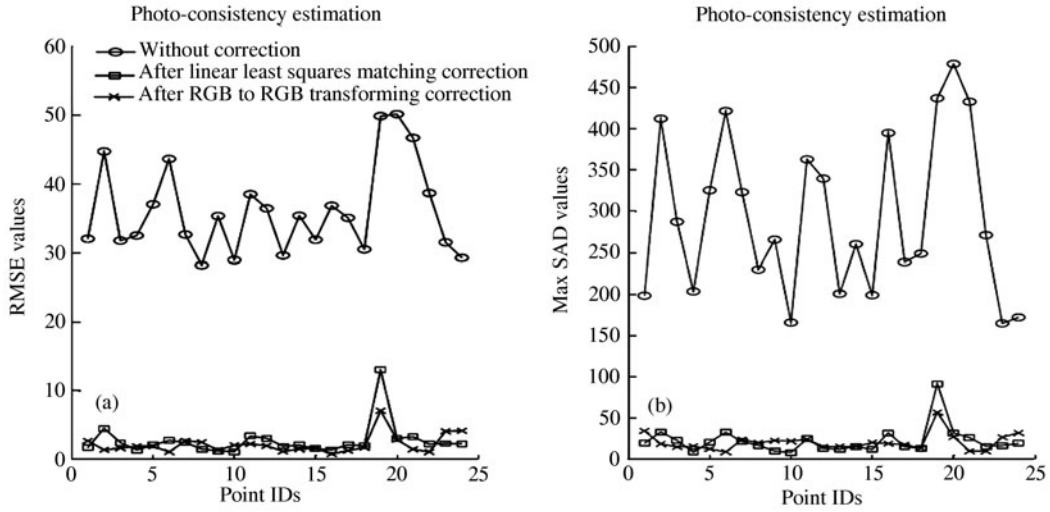

Figure 9 Photo-consistency matching costs before and after color calibration, plotted with respect to the sample number in color chart. (a) Comparison of RMSE (root mean square error) matching costs of six images; (b) comparison of the maximum SAD (sum of absolute distance) matching cost across each two images. Photo-consistency matching noises are significantly decreased after our color calibration. The 19th sample reaches the maximum cost value, which is used as photo-consistency check threshold.

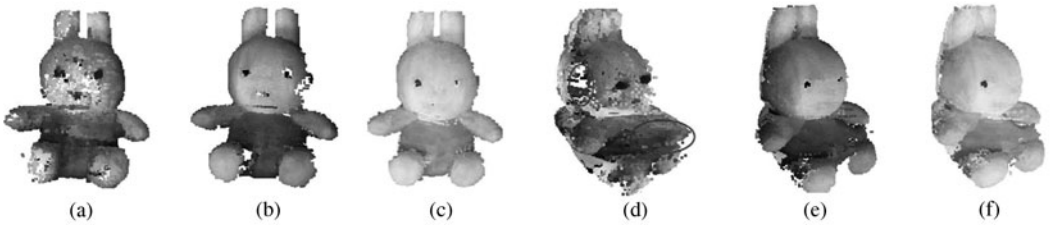

Figure 10 Space carving [8] reconstruction of a toy rabbit. (a) and (d): Reconstruction with original images shown in Figure 6. The threshold is set to 50 according to Figure 8(a). The appearance looks ugly due to the inconsistent colors. Space carving algorithm hardly works and geometry model is just the same as visual hull. Wrongly reconstructed regions are marked by circle. (b) and (e): Reconstruction with calibrated images shown in Figure 7. The threshold is set to 16. The artifacts are eliminated. (c) and (f): Reconstruction with calibrated images processed by a new response function mapping.

produce similar matching costs. The 19th sample exactly refers to the white block in the color chart and has the largest value. It means that the white color is the most ambiguous color of which photo-consistency matching cost can be used as the threshold for multiview reconstruction algorithms.

Figure 10 shows the space carving reconstruction results of the toy rabbit images before and after our color calibration with auto-determined thresholds (separately set to 50 and 16 according to the largest RMSE values in Figure 9(a)). Because of inconsistent colors in Figure 6, space carving algorithm hardly reconstruct the photo-consistency results and even wrongly remove lots of "correct" regions on surface, shown in Figure 10(a) and (d). After color calibration, Figure 10(b) and (e) show a more reasonable reconstruction result without noticeable artifacts. Additionally, we generate a set of images with a new response function and reconstruct with them for better appearances (Figure 10(c) and (f)). We conclude that photo-consistency based reconstruction results can be improved by our color calibration, even using multiple cameras with different settings and types.

6 Conclusion

We have presented a novel radiance-based color calibration method to improve photo-consistency estimation result for multi-camera vision system. Our method is software-based and independent of camera

settings and types, which implements a two phase process: response function and transformation matrix recovery, followed by color correction for multiple images. The calibrated images are consistent both visually and numerically. We also found that the white color is the most ambiguous color of which photo-consistency matching cost can be as the threshold for image-based modeling algorithms.

In this work, our effort is devoted to design a color calibration method without hardware parameter adjustment, whereas pixel truncation problem might affect our calibration results. We have shown that our method is more robust than Porikli 128s software-based method and presented some criteria to decide whether the truncation problem would occur. In future, we will try to remove other hardware dependences, such as color chart and a set of images with varying exposures. We think that the most potential application using our method is multi-camera remote immersion system.

Acknowledgements

The work was supported by National Basic Research Program of China (Grant No. 2009CB320805), National Science Foundation of China (Grant Nos. 61073070, 61170188), and Fundamental Research Funds for the Central Universities of China. The author would like to thank Liu Ke and Dong Zhao (The Chinese Academy of Sciences), Wu Xianyuan and Wang Feng (The Capital Normal University) for their useful suggestions during every week discussion.

References

1 Allard J, Menier C, Raffin B, et al. Grimage: markerless 3d interactions. In: ACM SIGGRAPH 2007. New York: ACM Press, 2007. 9–12
2 Zhao Q P. A survey on virtual reality. Sci China Ser F-Inf Sci, 2009, 52: 348–400
3 Kanade T. The 3d Room: Digitizing Time-Varying 3d Events by Synchronized Multiple Video Streams. Robotics Institute Technical Report. 1998
4 Hu Y, Qi Y, Tong X. Image-based modeling of inhomogeneous single-scattering participating media. Sci China Inf Sci, 2010, 53: 1141–1150
5 Pollefeys M, van Gool L, Vergauwen M, et al. Visual modeling with a hand-held camera. Int J Comput Vision, 2004, 59: 207–232
6 Hernandez C. Stereo and silhouette fusion for 3D object modeling from uncalibrated images under circular motion. Ph.D. thesis. Paris: Ecole Nationale Superieure des Telecommunications, 2004. 119–120
7 Seitz S M, Curless B, Diebel J, et al. A comparison and evaluation of multi-view stereo reconstruction algorithms. In: Proceedings of Conference on Computer Vision and Pattern Recognition. New York: IEEE Computer Society Press, 2006. 519–528
8 Kutulakos K N, Seitz S M. A theory of shape by space carving. Int J Comput Vision, 2000, 38: 199–218
9 Vogiatzis G, Hern C, Esteban N, et al. Multiview stereo via volumetric graph-cuts and occlusion robust photo-consistency. IEEE Trans Pattern Anal, 2007, 29: 2241–2246
10 Ilie A, Welch G. Ensuring color consistency across multiple cameras. In: Proceedings of the 10th IEEE International Conference on Computer Vision. Beijing: IEEE Computer Society Press, 2005. 1268–1275
11 Nanda H, Cutler R. Practical Calibrations for a Real-Time Digital Omnidirectional Camera. Computer Vision and Pattern Recognition Technical Sketches Report. 2001
12 Porikli F. Inter-camera color calibration by correlation model function. In: IEEE International Conference on Image Processing. Barcelona: IEEE Computer Society Press, 2003. 133–136
13 Joshi N. Color calibration for arrays of inexpensive image sensors. Master thesis. California: Stanford University, 2004. 10–13
14 Malik R, Bajcsy P. Achieving color constancy across multiple cameras. In: Proceedings of the 17th ACM International Conference on Multimedia. New York: ACM Press, 2009. 893–896
15 Yamamoto K, Oi R. Color correction for multi-view video using energy minimization of view networks. Int J Autom Comput, 2008, 5: 234–245
16 Chakrabarti A, Scharstein D, Zickler T. An empirical camera model for internet color vision. In: British Machine Vision Conference. London: Springer, 2009. 1–11
17 Mitsunaga T, Nayar S K. Radiometric self calibration. In: Proceedings of IEEE Computer Society Conference on Computer Vision and Pattern Recognition. Fort Collins: IEEE Computer Society Press, 1999. 274–380
18 Manders C, Aimone C, Mann S. Camera response function recovery from different illuminations of identical subject

matter. In: Proceedings of the International Conference on Image Processing. Singapore: IEEE Signal Processing Society Press, 2004. 2965–2968
19 Lin S, Gu J, Yamazaki S, et al. Radiometric calibration from a single image. In: Proceedings of IEEE Conference on Computer Vision and Pattern Recognition. Washington DC: IEEE Computer Society Press, 2004. 938–945
20 Mitsunaga T. RASCAL software. Http://www.cs.columbia.edu/CAVE/software/rascal/rrslrr.php
21 X-Rite Inc. ColorChecker classic product. Http://www.xrite.com/product overview.aspx?ID=820
22 Bouguet J Y. Camera calibration toolbox for MATLAB. Http://www.vision.caltech.edu/bouguetj/calib_doc
23 Point Grey Research Inc. Point grey flea2 product. Http://www.ptgrey.com/products/flea2/index.asp
24 ALLIED Vision Technologies. AVT marlin product. Http://www.alliedvisiontec.com/apac/products/cameras/firewire/marlin.html